Reaction Kinetics, Mechanisms and Catalysis (2021) 133:579–600
https://doi.org/10.1007/s11144-021-02008-6

The most reactive iron and manganese complexes with *N*-pentadentate ligands for dioxygen activation—synthesis, characteristics, applications

Katarzyna Rydel-Ciszek[1]

Received: 8 April 2021 / Accepted: 3 June 2021 / Published online: 15 June 2021

Abstract

The iron and manganese complexes that activate oxygen atom play multiple role in technologically relevant reactions as well as in biological transformations, in which exist in different redox states. Among them, high-valent oxo intermediate seems to be the most important one. Iron, and/or manganese-based processes have found application in many areas, starting from catalysis and sustainable technologies, through DNA oxidative cleavage, to new substances useful in chemotherapeutic drugs. This review is not only the latest detailed list of uses of homogeneous *N*-pentadentate iron and manganese catalysts for syntheses of valuable molecules with huge applications in green technologies, but also a kind of "a cookbook", collecting "recipes" for the discussed complexes, in which the sources necessary to obtain a full characterization of the compounds are presented. Following the catalytic activity of metalloenzymes, and taking into account the ubiquity of iron and manganese salts, which in combination with properly designed ligands may show similarity to natural systems, the discussed complexes can find application as new anti-cancer drugs. Also, owing to ability of oxygen atom to exchange in reaction with H_2O, they can be successfully applied in photodriven reactions of water oxidation, as well as in chemically regenerated fuel cells as a redox catalyst.

✉ Katarzyna Rydel-Ciszek
kasiar@prz.edu.pl

[1] Department of Physical Chemistry, Faculty of Chemistry, Rzeszów University of Technology, al. Powstańców Warszawy 6, P.O. Box 85, 35-959 Rzeszów, Poland

Graphical abstract

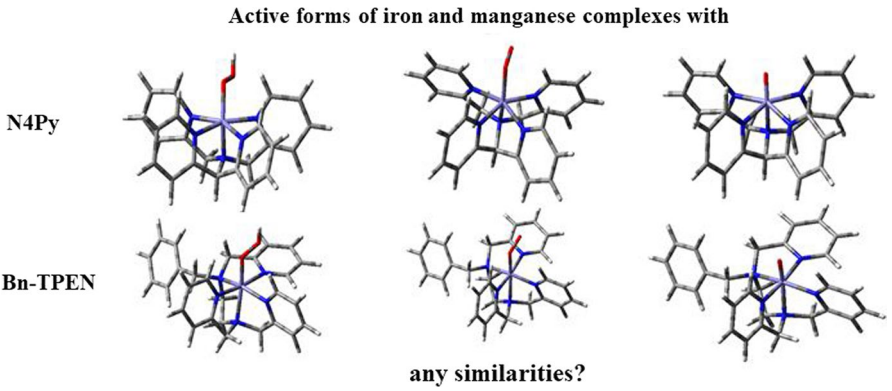

Keywords Bn-TPEN · Homogenous catalysis · Iron and manganese *N*-pentadentate catalysts · N4Py

Abbreviations

N4Py	*N,N*-Bis(2-pyridylmethyl)-*N*-bis(2-pyridyl)methylamine
N4Py*	N,N-bis(2-pyridylmethyl)-1,2-di(2-pyridyl)ethylamine
Bn-TPEN	*N*-Benzyl-*N,N′,N′*-tris(2-pyridylmethyl)ethane-1,2-diamine
BLM	Bleomycin
PhIO	Iodosylbenzene
OTf	$CF_3SO_3^-$
TFE	Tetrafluoroethylene
LS	Low-spin
HS	High-spin
MeCN	Acetonitrile
MeOH	Methanol
OAT	Oxygen atom transfer
HAT	Hydrogen atom transfer

Introduction

Mononuclear iron and manganese centers are common in oxygenases [1, 2]. Recently, synthesis of low-valent iron and manganese complexes capable of stabilizing intermediates produced in the oxygenation cycles, which show similarity to natural systems, is of great interest. Within the last two decades, a number of mononuclear complexes with oxoiron(IV) [3–20] and oxomanganese(IV) [9, 11, 18, 21] units supported by polydentate non-heme ligands have been investigated. These complexes serve as models for high-valent intermediates in the catalytic cycles of enzymes that carry out a series of oxidative modifications. Iron(IV)-oxo complexes as active oxidants were recognized in: α-ketoglutarate dioxygenase, halogenase

[22–25], and/or methane monooxygenase [22, 23]. These intermediates were identified with different spectroscopic techniques, on the basis of which it was founded that, they have a high-spin [spin (S) = 2] iron(IV)-oxo centre and the bond between the oxygen atom and iron ion shows double bond feature [24]. Furthermore, high-valent iron and manganese oxo complexes, produced in the reaction of water oxidation, were determining species in the "oxygen-evolving complex" (OEC) in photosystem II [4, 7, 26]. Manganese also plays an important role in many biological processes in which, similarly to iron, is present in different oxidation states. In organisms, the manganese-containing ribonucleotide reductases catalyze the transformation of ribonucleotides to deoxyribonucleotides, which is a preliminary step in DNA repair and replication [27]. Following the structure of enzymes, in laboratory conditions, complexes imitating the structure of their active centers were synthesized. Particularly effective for this purpose are ligands constructed with a fivefold pyridine donor set. Pentadentate ligands can be assigned into eight subgroups, this division is related with the binding each of the five *N*-donors to the central atom [28]. Based on article [28], there are known: ligands with linear network of five nitrogen atoms, tetracyclic ligands with a linked one *N*-donor side ring, tricyclic ligands with linked two *N*-donor side rings (three subgroups related with the position of two "pendant" donors), tetrapodal ligands, such as N4Py, elongated tripodal ligands like TPMEN, and moreover macrocyclic ligands [28–30]. Iron and manganese complexes containing pentadentate ligands are also broadly used as oxidants in many areas, e.g. biotechnology, synthesis of organic compounds, transformation of organic compounds, pharmacy as components that react with DNA [31–35]. These complexes have been successfully used as photosensitizers in solar cells and in redox and catalytic light-controlled processes.

N-pentadentate non-heme iron and manganese complexes characterization

Iron complex with N4Py ligand (Fig. 1a) and its oxygen adducts are perhaps the most extensively studied of the non-heme complexes. In 1999, Feringa, Que et al. [36] investigated a non-heme mononuclear iron(II) complex with N4Py ligand

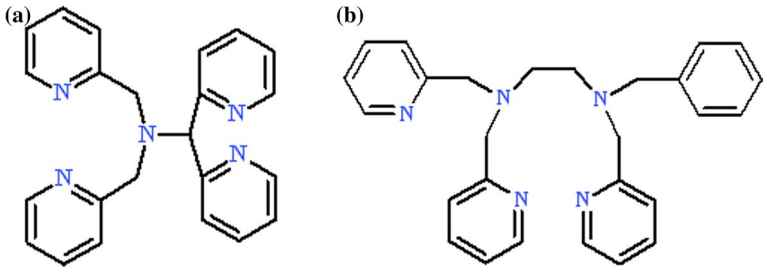

Fig. 1 Structural formulas of *N*-pentadentate ligands discussed in this work, **a** N4Py, **b** Bn-TPEN (hydrogen atoms were omitted)

{NMR data – [37]} to gain more information about the formation and stability of non-heme iron(III) hydroperoxo intermediates.

$[(N4Py)Fe^{II}(MeCN)]^{2+}$ (**1**) is formed as a dark red crystalline solid, with high yield in reaction of N4Py and $Fe(ClO_3)$ [as well as $Fe(ClO_2)$], in a methanol/acetonitrile solution, and was characterized by ^1H NMR, UV/Vis [37], ES/MS [30] techniques, moreover iron-N4Py complex can also be obtained by reacting with another iron salt – $Fe(OTf)_2{\cdot}2MeCN$ [17]. Cyclic voltamperograms of (**1**) indicates a reversible oxidation peak [at 0.99 V (*vs*. SCE)] associated with the Fe^{II}/Fe^{III} couple, and probably presenting the thermodynamic stability of the iron(II) complex [37]. The X-ray structure of this complex specify that iron centre is a six-coordinate ones; the *N*-pentadentate ligand saturates five iron coordination sites, leaving one free binding site to an acetonitrile molecule, which can simply be displaced by, for example, dioxygen. The $[(N4Py)Fe^{II}]^{2+}$ complex, due to the similarity in structure, is known as a synthetic model for iron bleomycin (BLM), on the other hand the BLM ligand, has been proposed to be an intermediate between heme and non-heme chemistry [38]. Iron-bleomycin, metalloglycopeptide clinically used in anti-cancer therapy [39–41], in the presence of dioxygen can trigger selective oxidative DNA cleavage [31, 33, 35, 42, 43]. The antitumor drug BLM is proposed to act via a low-spin iron(III) hydroperoxide intermediate called "activated bleomycin" [44]. Iron(II) complex with N4Py (**1**) due to the short Fe–N bond with a length of 1.91–1.96 Å is a low-spin (LS) one [37]. In reaction with H_2O_2 it turns into purple compound $[(N4Py)Fe^{III}(OOH)]^{2+}$ (**2**) named "purple intermediate" [37], which is capable of oxidizing various organic substrates [28, 44–47]. However, formation of (**2**) is closely dependent on used solvent e.g. in acetonitrile, the $[(N4Py)Fe^{III}(OOH)]^{2+}$ complex is obtained only in huge excess (> 50 equiv) of hydrogen peroxide, while in methanol, reaction with H_2O_2 is very fast, and only 1.2–2 equivalents of H_2O_2 are required to produce (**2**) [47]. Intermediate (**2**) (specified by EPR spectra, where $g = 2.17$, 2.12, 1.98 [37]) have also low-spin iron(III) centers ($S = 1/2$), showing charge-transfer bands near the 500–600-nm region related with transition hydroperoxo-to-iron(III). Their $\nu_{O\text{-}O}$ frequencies occurring near 800 cm^{-1} in the Raman spectrum, are lower than those obtained for their high-spin (HS) analogues [30]. (**2**) was also analyzed with techniques such as Raman {bands at 632 cm^{-1} (corresponding to strong Fe–O bond) and ~ 790 cm^{-1} (related with weak O–O bond) [30, 38, 45]}, ES/MS {$m/z = 555$ – $\{[(N4Py)Fe(OOH)]ClO_4\}^+$; $m/z = 753$ – $\{[(N4Py)Fe(OOH)](ClO_4)_3\}^-$ [36, 37]}, or by the use of DFT calculations {average of distances: r(Fe–O): 1.804, r(O–O): 1.490, r(Fe-N_{tr}): 2.033, r(Fe-N_c): 1.996 [45]}. The formation of (**2**) undergoes via two stages. In the first one, the addition of hydrogen peroxide to acetonitrile solution containing (**1**) causes the formation of $[(N4Py)Fe^{III}\text{-}OH]^{2+}$ complex ($g = 2.41$, 2.15, 1.92 specified by EPR spectra [30]); in the second stage – hydroperoxide group from H_2O_2 takes the place of hydroxide to form (**2**) [30, 38, 48]. $[(N4Py)Fe^{III}(\eta^1\text{-}OOH)]^{2+}$ can be converted to its conjugate base called "blue intermediate", which is a high-spin iron(III) adduct (with $S = 5/2$), in which the peroxo group is a side ligand, $[(N4Py)Fe^{III}(\eta^2\text{-}O_2)]^+$ [30, 49]. In Raman spectroscopy HS iron(III)-peroxo complexes, often show bands at 400–500 cm^{-1} region and in the 815–900 cm^{-1} area singed to $\nu_{Fe\text{-}O}$ and $\nu_{O\text{-}O}$ features, respectively. $[(N4Py)Fe^{III}(\eta^2\text{-}O_2)]^+$ is characterized by Raman (495 and 827 cm^{-1}), UV/Vis [methanol

λ_{max} (ε) = 685 nm (520 $M^{-1} \cdot cm^{-1}$)], EPR (g = 8.00, 5.60, 4.30) and MS (m/z = 455 – {[(N4Py)Fe(OO)]}$^{+}$) spectroscopy; also DFT geometry optimization was used for this complex and metal–ligand distances (Å) have been defined as: Fe–O, 1.96; Fe-N_{py}, 2.17 and 2.27, Fe-N_{amine}, 2.39 [30]. Unfortunately, [(N4Py)Fe^{III}(η^2-O_2)]$^{+}$ is unable to catalyze the hydrogen atom transfer (HAT) reaction [30]. In contrast, the "purple intermediate" (**2**) is capable of HAT reaction and has been proposed to be a precursor in the catalytic cycle for the generation of high-valent intermediates [36]. Raman studies of [(N4Py)Fe^{III}(OOH)]$^{2+}$ indicated a weakened O–O bond in the complex, so homolysis of the O–O bond of (**2**) can produce [(N4Py)Fe^{IV} = O]$^{2+}$ (**3**) intermediate [30, 38, 45]. Additionally, the green complex (**3**), oxo type, can be generated at room temperature in reaction with an excess of peracid or iodosylbenzene (PhIO), displaying considerable thermal stability and its shelf life is in the order of several days ($t_{1/2}$ = 60 h) [50, 51]. The stability of iron(IV)-oxo species is dependent on the pH of reaction solutions, complex (**3**) is stable at low pH (in the region of 5–6) but it decays rapidly as the pH of the reaction solutions increases [52]. Thus, (**3**) belongs to an rising class of Fe^{IV} = O non-heme complexes, with a near-IR spectral signature [optical d-d transition between 800 nm and 900 nm, related to green colour of (**3**)], as well as Raman spectra between 750 cm^{-1} and 850 cm^{-1} [13, 51], with a short Fe–O distance of ~ 1.64 Å [50], which makes it similar to oxoiron(IV) porphyrin species [53]. The oxidation state of the iron central atom can be determined by the use of advanced techniques such as Mössbauer, X-ray absorption near edge spectroscopy (XANES) [22, 24] or/and ^{1}H NMR [50]. The high oxidative power of (**3**) was suggested not only by catalytic research [54, 55] but also by theoretical studies [56, 57]. Based on density functional theory (DFT) calculations, it was found, that in case of complexes of iron(IV)-oxo, those with S = 2 have π * and σ * paths enabling the oxidation of the C-H bond, and complexes with S = 1, in this reaction, can only use the π * path [58]. These paths have some geometrical limitations – the σ* path is the most favorable when C-H bond, of organic compounds, approaches Fe = O species along the Fe–O axis, and the π* path is the most possible when C-H is upcoming under 120° with respect to Fe = O center [58]. The DFT calculations of reaction of cyclohexane hydroxylation by the complex [(N4Py)Fe^{IV} = O]$^{2+}$ were performed [56]. The triplet is the ground state, but it is also possible for this complex to occur in both a quintet and a singlet states [56]. Based on the DFT calculations, in which the reaction of oxidation of cyclohexene to alcohol catalyzed with a non-heme complex (**3**) was analyzed, Shaik et al. comparing [(N4Py)Fe^{IV} = O]$^{2+}$ with Cpd I cytochrome P450, showed that (**3**) is more reactive and exhibit a distinct solvent effect [56]. Additionally, some information regarding oxidation capacity of Fe^{IV} = O complexes were obtained on the basis of electrochemical research. Collins, Que et al. carried out bulk electrolysis in aqueous/MeCN to generate (**3**) from its iron(II) precursor [6]. Electrolysis at potentials above + 0.61 V generated [(N4Py)Fe^{III}(OH)]$^{2+}$, (UV/Vis – yellow chromophore, λ_{max} = 320 nm), at higher potentials the yellow solution was converted to the green one (λ_{max} = 695 nm) characteristic to (**3**) [6]. This positive redox potential explains the greater alkane oxidation reactivity of [(N4Py)Fe^{IV} = O]$^{2+}$ [22].

The Bn-TPEN (*N*-benzyl-*N*,'*N*',*N*'-tris(2-pyridylmethyl)-1,2-diaminoethane) {NMR data – [59]} is also *N*-pentadentate ligand (Fig. 1b), where individual

proportions of pyridine and amine groups allow for precise adjustment of properties and stability of iron complexes, and its $[(\text{Bn-TPEN})\text{Fe}^{\text{II}}]^{2+}$ (**1′**) complex is very similar to (**1**). $[(\text{Bn-TPEN})\text{Fe}^{\text{II}}(\text{OTf})](\text{OTf})$ is formed with high yield as a yellow powder in a reaction of Bn-TPEN ligand with $\text{Fe}(\text{OTf})_2{\cdot}2\text{MeCN}$ in a dichloromethane solution [17, 51]. There is also known the reaction of Bn-TPEN with either iron(II) or iron(III) chloride in dry methanol, followed by addition of a salt of the counter anion (ClO_4^-), leading to precipitation of yellow $[(\text{Bn-TPEN})\text{FeCl}]ClO_4$ and $[(\text{Bn-TPEN})\text{FeCl}](ClO_4)_2$ complexes [59]. It is interesting that, in the case of iron(II) complexes their spin states are closely related to the solvent used for the research. In acetonitrile, low-spin iron(II) complexes are preferentially formed, and high-spin ones – in acetone [36]. This observations was confirmed by ^{1}H NMR spectroscopy [60]. Measurements performed using cyclic voltammetry as a technique, indicated that for iron(II) complexes their redox potentials $\text{Fe}^{\text{III/II}}$ for those with LS are much higher, than for those with HS. In MeCN solutions the iron(II) complexes reveal reversible redox behaviour, while in MeOH – irreversible. In acetonitrile higher potentials of iron(II) complexes LS are observed [$E^{0'} = 1.00$ V for (**1**) and 0.95 V and for (**1′**) *vs* SCE], whereas in methanol for HS – lower ones [$E_{pc} = 0.29$ V, $E_{pa} = 0.63$ V for (**1**) and $E_{pc} = 0.29$ V, $E_{pa} = 0.75$ V for (**1′**) *vs* SCE] [60]. It is very important that the solvent (e.g. alcohol) plays an invaluable role in the formation of iron(III) complexes type hydroperoxo, both in the case of complexes (**1′**) and (**1**). Both these complexes can be used for dioxygen activation. In first step of this reaction, the high-spin iron(II) complex reacts with dioxygen to form an iron(III)-superoxo adduct, which in further transformations gives the low-spin hydroperoxo complex of iron(III) [60]. The coordinative saturated $S = 1/2$ $[(\text{Bn-TPEN})\text{Fe}^{\text{III}}(\text{OOH})]^{2+}$ (**2′**) species, can be produced, also in the reaction with excess hydrogen peroxide in hydroxylic solvents in the form of purple species stable for hours, named "sluggish oxidant" that undergoes via homolysis of the O–O bond [3]. Formation of (**2′**) in the presence of H_2O_2 occurs, analogous to (**2**), in two stages. Jensen et al. [59] assigned peaks of purple solutions observed in the ESI mass spectra to $[(\text{Bn-TPEN})\text{Fe}^{\text{III}}(\text{OOH})]^{2+}$ and $[(\text{Bn-TPEN})\text{Fe}(\text{OO})]^{+}$ complexes. In the spectra of "blue solutions", an intense *m/z* signal at 256 and a weak signal at *m/z* 511 were obtained for the acid–base equilibrium. Usually the most intense peak belongs to the ferryl species of $[(\text{Bn-TPEN})\text{Fe}^{\text{IV}}{=}\text{O}]^{2+}$ complex. Collision activated dissociation (CAD) of the ion at *m/z* 256 gives ions at *m/z* 248, 240 and 195, assigned to respectively ferryl species $[(\text{Bn-TPEN})\text{Fe}^{\text{IV}}{=}\text{O}]^{2+}$, ferrous species $[(\text{Bn-TPEN})\text{Fe}^{\text{II}}]^{2+}$, and to $[(\text{Bn-TPEN})\text{Fe}^{\text{II}}\text{-}C_7H_6)]^{2+}$ [59]. EPR analysis confirmed (**2′**) as low-spin Fe(III) complex – $[(\text{Bn-TPEN})\text{Fe}^{\text{III}}(\eta^1\text{-OOH})]^{2+}$ ($g = 2.20$, 2.16, 1.96). After addition of base to high-spin iron(III) blue solutions of $[(\text{Bn-TPEN})\text{Fe}^{\text{III}}(\eta^2\text{-}O_2)]^{+}$ new signals (at $g = 7.60$ and 5.74) is produced [59]. Treatment of (**1′**) with excess solid PhIO in MeCN at 25 °C provides a green compound $[(\text{Bn-TPEN})\text{Fe}^{\text{IV}}{=}\text{O}]^{2+}$ (**3′**) with λ_{max} at 739 nm and a shoulder near 900 nm, but this species is less stable (about ten times) than (**3**) ($t_{1/2} = 6$ h) [17, 51]. Monocrystals of (**3′**) have not been separated yet, therefore information on its structure should be obtained by alternative methods [50]. Complex (**3′**) was characterised by ES/MS spectroscopy [51, 59], X-ray crystallography [22, 50] or EXAFS analysis [22]. The ligand flexibility

indicates the possibility of the formation of three isomers: A, B and C—differing in the position and number of pyridine rings, at a given position relative to the Fe–O axis (pyridine rings can eclipse Fe–O axis, can be perpendicular to the axis, or can coordinate to the oxygen atom in the trans position) [50]. Analysis of the ^{1}H NMR spectrum of (**3′**) implies that the Bn-TPEN ligand in complex with iron ions has an A-isomer structure—with one pyridine ring located perpendicular to the Fe–O axis and two pyridine rings eclipse on this axis [50]. Those observation were also confirmed by theoretical research. Considering the DFT calculations of (**3′**), isomer A was found to be the most stable and the average distance of each Fe–N bond was approximately 2.040 Å. Comparing this catalyst with an analogous complex but build with the N4Py ligand, which in turn obtains excellent stabilization because, it has four *N*-rings situated parallel to the Fe = O line (the average Fe–N bond distance is 2.00 Å), explains why half-life of (**3**) is longer than (**3'**) [50]. Based on electrochemical measurements, the half-wave potentials of (**3'**) was determined as one-electron reduction potentials equal to 0.49 V *vs* SCE. This approach allows to understand the mechanism of the demonstrated catalytic activity, assuming the possibility of electron transfer (ET) reactions of iron(IV)-oxo complexes with N4Py and Bn-TPEN, originally adopted by Lee et al. [61]. They demonstrated that the reorganization energies of the electron-transfer (ET) reduction of complexes (**3'**) and (**3**) increase (Bn-TPEN, 2.55 eV < N4Py, 2.74 eV), when one-electron reduction potentials (E_{red}) is shift in positive site (Bn-TPEN, 0.49 V < N4Py, 0.51 V *vs* SCE). It can be assumed that the higher E_{red} of $Fe^{IV} = O$ complexes is achieved by compensating for the greater reorganization energy, which includes the corresponding structural change needed for the electron relocate reaction. Flexible non-heme ligand compared to the inflexible heme ligand allows for greater reorganization ofthe bond after ET reduction, which may be connected with higher reorganization energies values [61].

Steric and electronic aspects of the ligands N4Py and Bn-TPEN, and their complexes with iron, along with the fact of low toxicity of manganese compounds compared to iron [62], encouraged me to focus my attention on this kind of manganese complexes with *N*-pentadentate ligands. Table 1 presents a selected spectroscopic properties of both iron and manganese complexes.

Yellow microcrystals of the complex $[(N4Py)Mn^{II}]^{2+}$ (**4**) were obtained by the reaction of the $Mn^{II}(OTf)_2$ salts and N4Py ligand in acetonitrile under an Ar atmosphere [26, 63]. The complex was analysed with mass spectrometry using ESI (ESI–MS), UV/Vis spectroscopy, along with the X-ray diffraction (XRD) technique or DFT calculations [26, 63].

It was reported that peroxomanganese(III) adduct can be produced both in reaction with KO_2 and H_2O_2, so for generation of $[(N4Py)Mn^{III}(O_2)]^{+}$ complexes the excess of KO_2 in MeCN solutions was used [64]. A "blue solution" with a prominent peak at *m/z* 454 in an ESI–MS experiment, consistent with its formation as $[(N4Py)Mn^{III}(O_2)]^{+}$ was obtained [64]. Kaizer et al. [65] presented that using water as the reaction environment, non-heme manganese(IV)-oxo complexes showed similarity to the reaction of catalase. $N4Py^{*}$ manganese(II) ion complexes, similar to $[(N4Py)Fe^{II}]^{2+}$, can directly react with hydrogen peroxide to give $Mn^{III}OOH$, and then the homolytic cleavage of O–O results in the formation of manganese(IV)-oxo

Table 1 Selected spectroscopic properties of iron and manganese complexes with N4Py or/and Bn-TPEN ligands

Complexes	UV/Vis	References	EPR	References	ES-MS	References
$[(N4Py)Fe^{II}]^{2+}$	Acetone: λ_{max} (ε) = 382 nm (5700 $M^{-1}{\cdot}cm^{-1}$), 458 nm (4000 $M^{-1}{\cdot}cm^{-1}$)	[37]	EPR-silent	[33, 36]	*m/z* = 520 $\{[(N4Py)Fe^{II}](ClO_4)(MeCN)\}^+$ *m/z* = 210 $\{[(N4Py)Fe^{II}](2ClO_4)(MeCN)\}^{2+}$ *m/z* = 522 $\{[(N4Py)Fe^{II}](ClO_4)\}^+$	[30] [33]
$[(N4Py)Fe^{III}(OOH)]^{2+}$	Acetone: λ_{max} (ε) = 530 nm (1100 $M^{-1}{\cdot}cm^{-1}$) MeOH: λ_{max} (ε) = 548 nm (1100 $M^{-1}{\cdot}cm^{-1}$)	[36–38] [36, 45]	*g* = 2.17, 2.12, 1.98	[36, 37]	*m/z* = 555 $\{[(N4Py)Fe^{III}(OOH)](ClO_4)\}^+$ *m/z* = 753 $\{[(N4Py)Fe^{III}(OOH)](ClO_4)_3\}^-$	[30] [36, 37]
$[(N4Py)Fe^{III}(OH)]^{2+}$	MeCN: λ_{max} = ~320 nm	[6]	*g* = 2.41, 2.15, 1.92	[36]	*m/z* = 539 $\{[(N4Py)Fe^{III}(OH)](ClO_4)\}^+$	[33]
$[(N4Py)Fe^{III}(\eta^2\text{-}O_2)]^+$	MeOH: λ_{max} (ε) = 685 nm (520 $M^{-1}{\cdot}cm^{-1}$)	[30]	*g* = 8.00, 5.60, 4.30	[30]	*m/z* = 455 $[(N4Py)Fe^{III}(OO)]^+$	[30]
$[(N4Py)Fe^{VI}{=}O]^{2+}$	MeCN: λ_{max} (ε) = 695 nm (400 $M^{-1}{\cdot}cm^{-1}$)	[6, 17] [51]	EPR-silent	[4]	*m/z* = 221 $[(N4Py)Fe^{VI}{=}O]^{2+}$ *m/z* = 538 $\{[(N4Py)Fe^{VI}{=}O](ClO_4)\}^+$	[7] [7, 51]
$[(Bn\text{-}TPEN)Fe^{II}]^{2+}$	MeCN: λ_{max} (ε) = 322 nm (800 $M^{-1}{\cdot}cm^{-1}$), 401 nm (2050 $M^{-1}{\cdot}cm^{-1}$), 894 nm (17 $M^{-1}{\cdot}cm^{-1}$)	[49]	EPR-silent	[17, 49]	*m/z* = 240 $[(Bn\text{-}TPEN)Fe^{II}]^{2+}$ *m/z* = 628 $\{[(Bn\text{-}TPEN)Fe^{II}](OTf)\}^+$	[49, 59] [51]
$[(Bn\text{-}TPEN)Fe^{III}(OOH)]^{2+}$	MeCN: λ_{max} = 542 nm	[49]	*g* = 2.20, 2.16, 1.96	[49, 59]	*m/z* = 256 $[(Bn\text{-}TPEN)Fe^{III}(OOH)]^{2+}$	[59]
$[(Bn\text{-}TPEN)Fe^{III}(\eta^2\text{-}O_2)]^+$	MeCN: λ_{max} = 770 nm	[49]	*g* = 7.60, 5.74	[49, 59]	*m/z* = 511 $[(Bn\text{-}TPEN)Fe^{III}(OO)]^+$	[49, 59]
$[(Bn\text{-}TPEN)Fe^{VI}{=}O]^{2+}$	MeCN: λ_{max} (ε) = 739 nm (400 $M^{-1}{\cdot}cm^{-1}$)	[17, 51]	EPR-silent	[17]	*m/z* = ~249 $[(Bn\text{-}TPEN)Fe^{VI}{=}O]^{2+}$ *m/z* = 644 $\{[(Bn\text{-}TPEN)Fe^{VI}{=}O](OTf)\}^+$	[7, 59] [51]
$[(N4Py)Mn^{II}]^{2+}$	Acetate buffer: λ_{max} (ε) = ~260 nm (154 $M^{-1}{\cdot}cm^{-1}$)	[26]	EPR-silent	[71]	*m/z* = 457 $\{[(N4Py)Mn^{II}](Cl)\}^+$	[64]
$[(N4Py)Mn^{VI}{=}O]^{2+}$	CF_3CH_2OH-MeCN: λ_{max} = 940 nm CF_3CH_2OH: λ_{max} (ε) = ~940 nm (≈ 250 $M^{-1}{\cdot}cm^{-1}$)	[71] [63, 67]	*g* = 5.80, 3.20, 2.01	[71]	*m/z* = 220 $[(N4Py)Mn^{VI}{=}O]^{2+}$ *m/z* = 240 $\{[(N4Py)Mn^{VI}{=}O](MeCN)\}^{2+}$ *m/z* = 587 $\{[(N4Py)Mn^{IV}{=}O](OTf)\}^+$	[63]

Table 1 (continued)

Complexes	UV/Vis	References	EPR	References	ES-MS	References
$[(Bn\text{-}TPEN)Mn^{II}]^{2+}$	Acetate buffer: $\lambda_{max} = \sim 260$ nm MeCN/MeOH: $\lambda_{max} = \sim 260$ nm	[26] [84]	$g = 5.36, 3.60, 2.06$	[69]	$m/z = 239$ $[(Bn\text{-}TPEN)Mn^{II}]^{2+}$ $m/z = 627$ $\{[(Bn\text{-}TPEN)Mn^{II}](OTf)\}^{+}$	[69]
$[(Bn\text{-}TPEN)Mn^{VI}{=}O]^{2+}$	CF_3CH_2OH: λ_{max} (ε) = ~ 1040 nm (220 $M^{-1}{\cdot}cm^{-1}$)	[69]	$g = 5.53, 2.76, 1.76$	[69]	$m/z = 247$ $[(Bn\text{-}TPEN)Mn^{VI}{=}O]^{2+}$ $m/z = 643$ $\{[(Bn\text{-}TPEN)Mn^{IV}{=}O](OTf)\}^{+}$	[69]

compound [65]. The oxidative reactivity of manganese hydroperoxides, during the reaction with organic substrates was also investigated [66], but so far complexes such as $Mn^{III}OOH$ with N4Py and Bn-TPEN ligands are hardly characterized in literature.

As is the case of iron complexes with N4Py, the formations of a greenish-yellow $[(N4Py)Mn^{IV}=O]^{2+}$ species (**5**) can be generated by the reaction of (**4**) with PhIO – the characteristic absorption band at 950 nm, and weak signals at 600, 450 nm were observed. Interestingly, complex (**2**) is more stable in the air atmosphere ($t_{1/2}$ = 2.75 h) than under inert gas atmosphere ($t_{1/2}$ is about 0.5 h) [63]. The ESI–MS spectrum of (**5**) showed peaks at *m/z* = 220 {main peak related with $[(N4Py)Mn^{IV}=O]^{2+}$}, 240 {assigned to $[(N4Py)Mn^{VI}=O(MeCN)]^{2+}$} and 587 {connected with $[(N4Py)Mn^{IV}=O(CF_3SO_3)]^{+}$} [63]. A perpendicular mode X-band EPR spectrum of (**5**) is typical of a mononuclear, $S = 3/2$ Mn^{IV} ion [63], the spin state was confirmed using the modified NMR method [67]. Furthermore, a excited states with charge-transfer and ligand-field of (**5**) were defined using combined electronic absorption, variable-temperature magnetic circular dichroism spectroscopy and time-dependent DFT methods [68]. Chemical reactivity of (**5**) is similar to the one corresponding to manganese(IV)-oxo complex with the Bn-TPEN ligand [69].

The white solid complex $[(Bn\text{-}TPEN)Mn^{II}]^{2+}$ (**4′**) was synthesized in reaction of $Mn^{II}(CF_3SO_3)_2{\cdot}2MeCN$ [manganese(II) salt] with Bn-TPEN in MeCN under an inert atmosphere [26, 69]. On ESI–MS spectrum, peaks at *m/z* = 239 corresponding to $[(Bn\text{-}TPEN)Mn^{II}]^{2+}$ and at 627 related with $[(Bn\text{-}TPEN)Mn^{II}(CF_3SO_3)]^{+}$ were present [69]. Reaction (**4′**) with excess of iodosylbenzene led to the formation of a greenish-yellow complex (**5′**), with a characteristic band at 1040 nm [69]. The intermediate ($t_{1/2} \approx 40$ min at 25 °C) was characterized by X-band EPR (the presence of signals characteristic for Mn^{IV} with spin equal 3/2 was observed); ESI–MS {$[(Bn\text{-}TPEN)Mn^{IV}=O]^{2+}$ – signals correlate with $[(Bn\text{-}TPEN)Mn^{IV}=O]^{2+}$ at *m/z* = 247 and $[(Bn\text{-}TPEN)Mn^{IV}=O(CF_3SO_3)]^{+}$ at *m/z* = 643 were obtained}; or EXAFS techniques [Mn = O bound is about 1.69 Å, what is comparable with (**5**)] [69].

Reactivity regulators of high-valent metal-oxo complexes

Inactive redox metal ions play a key role in controlling the reactivity of high-valent complexes with metal-oxo group in various chemical as well as enzymatic processes. Nam and Fukuzumi et al. [70] investigated the oxidative properties of $[(N4Py)Fe^{IV}=O]^{2+}$ (**3**) and established that, the outer non-redox metal ion, like e.g. Sc^{3+}, could significantly accelerate of the electron transfer reaction rate of the $Fe^{IV}=O$ oxidants, even to 10^8-fold. When the triflate scandium is present, the absorption bands due to (**3**) (λ_{max} = 695 nm) decrease, complexes $[(N4Py)Fe^{III}(O)]^{+}$-Sc^{3+} and $[(N4Py)Fe^{III}(O)]^{+}$-$(Sc^{3+})_2$ are formed, also for the Fe^{IV}/Fe^{III} pair the redox potential changes from + 0.51 to + 1.35 V (*vs* SCE) [70]. Furthermore, adding Sc^{3+} can shift the of sulfide oxygenation mechanism by (**3**) from oxygen to electron transfer [66]. Mononuclear non-heme $[(N4Py)Mn^{IV}=O]^{2+}$ can binds scandium ions; the addition of Sc^{3+} to (**5**) changed the absorption spectrum; the band at about 940 nm characteristic for (**5**) changed to a new

absorption band registered at 680 nm. During the reaction, such complexes as $[(N4Py)Mn^{IV}=O]^{2+}$-Sc^{3+} ($t_{1/2} \approx 12$ h at 25 °C) and $[(N4Py)Mn^{IV}=O]^{2+}$-$2Sc^{3+}$ ($t_{1/2} \approx 1$ day at 25 °C) were formed, the spin state of the Mn^{IV} is equeral 3/2 [67]. In oxidation reactions, the binding of Sc^{3+} ions has a large impact on the reactivity of the Mn(IV)-oxo complex. The effect includes an approximately 2200-fold increase in the rate of the thioanisole oxidation reaction (i.e., oxygen atom transfer—OAT), but also a decrease of about 180 times in the reaction of 1,4-cyclohexadiene (e.g. hydrogen atom transfer – HAT) [67]. Thus, Fukuzumi, Pushkarm, Nam et al. [67] demonstrated the first example of non-heme metal-oxo complex, additionally formed with redox inactive metal ions, which has an opposite effect on the reactivity of the oxo adduct in the OAT and HAT reactions. Research on tuning the reactivity of mononuclear non-heme manganese(IV)-oxo complexes were additionally carried out by Fukuzumi, Nam et al. [71]. They studied the impact of triflic acid (HOTf) on Mn^{IV}-oxo complexes, with both ligands (L = N4Py and Bn-TPEN). Reddish brown complexes of the structure $[(L)Mn^{IV}=O]^{2+}$-$(HOTf)_2$ were prepared in situ by addition of HOTf to $[(L)Mn^{IV}=O]^{2+}$ [71]. After addition of HOTf to complex (**5**) except the original absorption band (at about 940 nm), also a new one (at 550 nm, $\varepsilon = 540\ M^{-1}\cdot cm^{-1}$) was generated. Related changes in UV/Vis were also observed for (**5′**) (new peak at 580 nm, $\varepsilon = 600\ M^{-1}\cdot cm^{-1}$ was formed) [71]. Complexes with triflic acid are relatively stable at 0 °C [$t_{1/2} = 6$ h (for a complex with N4Py ligand) and $t_{1/2} = 1.5$ h (for a complex with Bn-TPEN)]. Binding of triflic acid to the oxo group of the $Mn^{IV}=O$ complex leads to shifts of the one-electron reduction potential towards more positive potentials and influences the inverse reactivity in OAT and HAT reactions. Comparing the complex $[(L)Mn^{IV}=O]^{2+}$ with $[(L)Mn^{IV}=O]^{2+}$-$(HOTf)_2$, it was found that, for complexes with two additionally bound HOTf groups, the reactivity in OAT reactions increased, but in HAT reactions slowdown was detected [71].

Ce^{III} ions can reversibly bind to complexes $[(N4Py)Fe^{IV}=O]^{2+}$, forming a compound of Fe^{III}-O-Ce^{IV} type, the equilibrium state of this reaction rely on the choice of solvents, and in fact on the MeCN/water ratio [72, 73]. Based on the research, it was found that Fe^{IV} and Ce^{IV} centers have similar reduction potentials. Moreover, the equilibrium contributes to a change in the spin state of the iron, from spin equal 1 observed in $[(N4Py)Fe^{IV}=O]^{2+}$ to spin equal 5/2 characterized for $[(N4Py)Fe^{III}$-O-$Ce^{IV}(OH_2)(NO_3)_4]^{+}$. Based on this, it can be assumed that Fe(IV)-oxo complexes may participate in multi-spin reactions [72, 73].

Iron high-valent adducts with nitride group may be present in various enzymes, for example in the nitrogenases and/or in cytochrome P450, but since they have not yet been isolated, little data is available on their oxidizing properties, or their structure. In laboratory conditions, iron complexes with the Bn-TPEN ligand were used to prepare models of iron(IV)-imido compounds [74]. Based on the conducted research it was found that the complex containing the Bn-TPEN ligand and the iron(IV)-tosylimido moiety, compared to the analogous compound, but containing the iron(IV)-oxo species in the center, shows unfortunately weaker oxidizing properties [74].

N-pentadentate iron and manganese complexes – recent trends in catalysis

In the chemical industry, it is important that the properly activated catalyst not only has high selectivity, but also shows precise and controlled reactivity. Moreover, in accordance with the principles of "green chemistry" the generated waste should be as little environmentally harmful as possible [75, 76]. The use of eco-friendly oxidants like dioxygen or hydrogen peroxide in broadly understood oxidation reactions is a subject of continued attention. Iron and manganese complexes with *N*-pentadentate ligands are of great interest and are the matter of many research works, therefore only the latest results of the reactions catalyzed by Fe and Mn complexes with N4Py and Bn-TPEN ligands will be discussed in this chapter (Table 2).

Recently iron *N*-pentadentate catalysts (**1**) were used in oxidation of cyclohexane to cyclohexanol and cyclohexanone by hydrogen peroxide [28]. The $[(N4Py)Fe^{II}]^{2+}$ complex, in the presence of aldehydes like benzaldehyde and isobutyraldehyde, as co-reductants, activates dioxygen and is able to purposefully and efficiently carry out Baeyer–Villiger reaction, in which oxidation of cyclohexanone derivatives to ε-caprolactones occurs [77], or similarly to iron(II) complexes with Bn-TPEN, can find application in chemically regenerated fuel cells as a redox catalyst (Scheme 1) [78].

In the diagram presented, a liquid phase redox mediator, that flows through the cathode and acts as an electron source is used, and iron(II)/(III) complexes with N4Py and/or Bn-TPEN are applied to the reduction of oxygen from air. Iron(II) complexes combine with the reduced form of the mediator to give iron(III) forms, which react with molecular oxygen to regenerate the iron(II) complex. Such a solution may contribute to the improvement of the functions of standard fuel cells, based on the cathodic oxygen reduction reaction. The introduction of FlowCath® technology with proton exchange membrane can be a competitive method, and consist in a usage of the cathode with the liquid catalyst regeneration system, which enables a significant reduction in platinum content and is associated with lower costs [78]. Moreover, complexes $[(N4Py)Fe^{IV}=O]^{2+}$ and $[(Bn\text{-}TPEN)Fe^{IV}=O]^{2+}$ can replace oxygen atom in reaction with H_2O [79], and with derivatives of *p*-benzoquinone as a plastoquinone counterpart, has been successfully used in the photodriven reaction of water oxidation [4]. Both N4Py and Bn-TPEN ligands produced highly reactive $Fe^{IV}=O$ complexes [63], with weaker solvent-interactions, and the Mn^{IV}-oxo units seems to be more basic than its Fe^{IV}-oxo analogues [11]. For the $Mn^{IV}=O$ adducts, DFT computations predicted that (**5**) has a larger barrier for H-atom abstraction from cyclohexane than (**5′**) [80]. The complexes (**5**) and (**5′**) can catalyse oxidation of olefins [81]. It is interesting that $[(N4Py)Mn^{II}]^{2+}$ shows the ability to oxidize H_2O to O_2 in the presence of Oxone® [82, 83] or hydrogen peroxide [82], which is important for research into manganese oxidants that can be used to oxidize water. Furthermore, non-heme coordination complexes of manganese, $[(N4Py)Mn^{II}]^{2+}$ and $[(Bn\text{-}TPEN)Mn^{II}]^{2+}$ catalyze the reaction in which chlorine dioxide is obtained from chlorite,

Table 2 Selected processes catalyzed by iron and manganese complexes with N4Py or Bn-TPEN

Catalyst system/oxidizer/solvent	Reaction	Reaction products with characteristic process parameters	References
$[(N4Py)Fe^{II}]^{2+}$ (0.01 mM)/O_2/MeCN	cyclohexanone derivatives (0.01 M) oxidation	*ε*-caprolactones; e.g. for cyclohexanone oxidation, with (0.15 M) benzaldehyde and/or *m*-chloroperoxybenzoic acid, yields 73% and 100%, respectively*	[77]
$[(N4Py)Fe^{II}]^{2+}$ (30 µM)/O_2/DMSO/H_2O	DNA cleavage	drug antitumor activity; e.g. 77 ± 4.2% of necrotic/late apoptotic SKOV-3 cells, (temp. 4, 37 °C)	[41]
$[(N4Py)Fe^{II}]^{2+}$ (0.2 mM)/plastoquinone analogs (0.50 mM)/H_2O (0.50 M) /MeCN	photodriven water oxidation	O_2, yield – almost 100%**	[4]
$[(N4Py)Mn^{II}]^{2+}$ (10 µM) or $[(Bn\text{-}TPEN)Mn^{II}]^{2+}$ (50 µM)/acetate buffer (50 mM)	catalytic formation of chlorine dioxide from chlorite (2–10 mM)	chlorine dioxide (for both catalysts – 31%)***	[26]
$[(N4Py)Mn^{II}]^{2+}$ (2–4 mM) /Oxone® or H_2O_2 (10 − 250 mM)/H_2O	oxygen evolution	O_2, e.g. for Oxone® – $V_{max} = 12.3 \pm 1.7$ [mol of O_2/(mol of Mn)/h] (temp. 25 °C)	[82]
$[(N4Py)Mn^{IV}=O]^{2+}$ (0.5 mM)/ CF_3CH_2OH /MeCN	cyclohexene (0.2 M), cyclooctene (0.1 M) oxidation	corresponding ketone, alcohol and/or epoxide; cyclohexenol (34%), cyclohexenone (6%), cyclohexene oxide (~6%) and cyclooctene oxide (91%), respectively (temp. 25 °C)	[81]
$[(Bn\text{-}TPEN)Mn^{II}]^{2+}$ (1 mM)/$Al(OTf)_3$ (2 mM) / MeCN/CH_2Cl_2	catalytic epoxidation of cyclooctene (0.05 M)	corresponding oxide (89%), (temp. 0 °C, time: 3.5 h)	[85]
$[(Bn\text{-}TPEN)Mn^{II}]^{2+}$ (0.5–10 mM)/air or O_2/MeCN and/or MeOH	cyclohexene (1–4 M) oxidation	corresponding ketone, alcohol, and epoxide; e.g cyclohexanone (12%), cyclohexenol (6%) and traces of epoxide****	[84]
$[(Bn\text{-}TPEN)Mn^{IV}=O]^{2+}$ (0.5–0.8 mM) /TFE/MeCN	anthracene (0.10 mM), 9-methylanthracene (0.20 mM), 9,10-dimethylanthracene (0.25 mM) oxidation	corresponding ketones – anthraquinones; e.g. anthracene was completely (100% yield) oxidized to anthraquinone (temp. 0 °C, time: ~50 min.)	[86]
$[(Bn\text{-}TPEN)Mn^{IV}=O]^{2+}$ (0.5 mM)/CF_3CH_2OH / MeCN	cyclohexene (0.2 M), cyclooctene (0.1 M) oxidation	corresponding ketone, alcohol and/or epoxide; cyclohexenol (26%), cyclohexanone (8%), cyclohexene oxide (18%) and cyclooctene oxide (94%), respectively (temp. 25 °C)	[81]

*The highest conversions after 15 h, at 60 °C

**Calculated on the basis of the introduced amounts of plastoquinone analogues, at 25 °C

***Calculated using the ratio of the final ClO_2 concentration to reacted chlorite concentration; for 4 mM $[ClO_2^-]_0$, at ambient temp

****Calculated on the basis of the introduced substrate concentration; for 1 mM catalyst in MeCN, 1 M substrate, after 24 h, under O_2 atmosphere, at ambient temp

and opens the door to new method of the preparation of chlorine dioxide, which can be used on site or in the preparation of ClO_2. They also eliminate the need for more expensive and complex higher molecular weight porphyrin ligands [26]. $[(Bn\text{-}TPEN)Mn]^{2+}$ catalyze oxidation of cyclohexene by dioxygen to ketone and alcohol [84], and epoxidation of cyclooctene, where redox-inactive metal ions, acting as a Lewis acid in oxygen atom transfer reaction were used [85]. However, when there are no redox-inactive metal ions in the reaction medium, then the manganese(II) catalyst reacts very sluggish, (8.7% yield of epoxide), and addition of Al^{3+} ions to manganese(II) complex significantly improves epoxidation (88.9% yield of epoxide) [85]. Recent reports on the non-heme synthetic $[(Bn\text{-}TPEN)Mn^{IV}=O]^{2+}$ complex revealed its capability to activate strong C-H bonds [86]. Manganese(IV)-oxo complexes (**5′**) and $[(Bn\text{-}TPEN)Mn^{IV}=O(Sc(OTf)_3)_2]^{2+}$ were used in reaction of anthracene, 9-methylanthracene and 9,10-dimethylanthracene oxidation to corresponding ketones (e.g. anthracene to anthraquinone) [86].

Oxidative DNA cleavage

In the case of iron complexes with Bn-TPEN, as well as with N4Py, studies of activity against human 20S proteasome were carried out. Both tested compounds were found to be effective inhibitors of the studied proteasome, and this information may be of use in further research on their anti-cancer activity. Moreover, it was found that iron complexes with N4Py or Bn-TPEN act according to other mechanisms, which may be respectively connecting to the enzyme or its oxidation [87]. Recently, the usage of the discussed complexes for oxidative DNA cleavage is limited to the ones based on iron, mainly supported on N4Py skeleton. Rots, Roelfes et al. showed that a combination of iron(II), zinc(II) or copper(II) compounds can be produced when N4Py is introduced to cell cultures, nevertheless it is possible that the metal ion will be further switched by other metal ions available in cells. In the reported research, complexes of Mn(II) ions and N4Py were also analyzed, but it was found that for coordination reasons [average length of the bonds between metal and N4Py nitrogen in the manganese(II) compounds is larger than the one in the iron(II) complexes; nevertheless the manganese(II) ions with analyzed *N*-pentadentate ligand indicate the most distorted structure] the formation of Mn(II)-N4Py is not privileged [31]. Moreover, Mn(II) ions are easily exchanged for Fe(II), yielding a stable complex $[(N4Py)Fe^{II}]^{2+}$, and only insignificant activity of manganese complexes in DNA cleavage reactions was found (Scheme 2). Also, based on a comparison of data obtained as a result of chemical and biological tests, it was suggested that (**1**) is a compound leading to oxidative destruction of cells. After the addition of free ligand (N4Py), high activity was found, which may be due to the combination of biological scavenging reactions with oxidative destruction reactions induced by the iron(II) complex [31].

The transition from the singlet state to the higher excited states is expected to occur via the triplet intermediate state, the triplet state would allow to a reaction with $^3O_2$, which initiates DNA cleavage by oxygen activated by $[(N4Py)Fe^{II}]^{2+}$. In aqueous solution of (**1**) the possibility of transition between singlet and, probably,

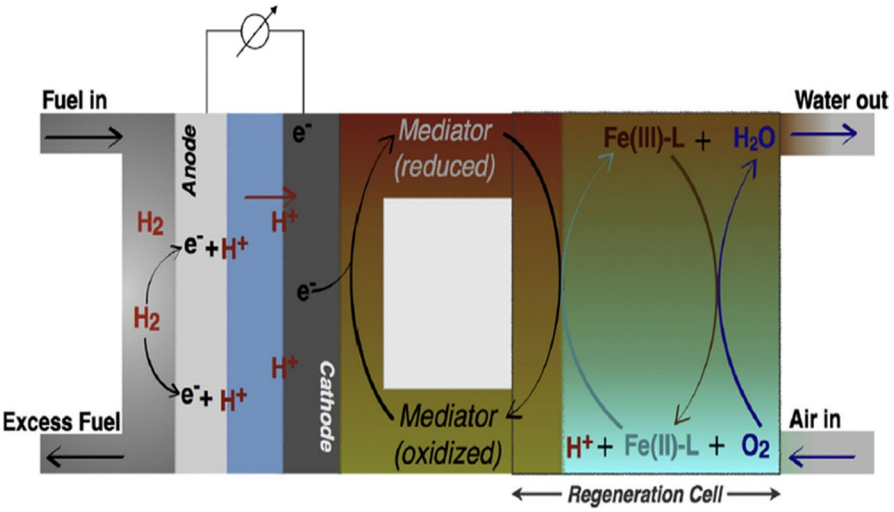

Scheme 1 Figure presenting, in a schematic manner, the principle of work of a Proton Exchange Membrane fuel cell employing the FlowCath® technology. An iron complex with *N*-pentadentate ligands like N4Py and/or Bn-TPEN, with an electron source mediator, is applied as a catalyst to reduce dioxygen, and is an alternative to the cathode dioxygen reduction reaction [78]. Reprinted from Elsevier Copyright© 1969, https://doi.org/10.1016/j.jpowsour.2018.07.056, further permissions related to Scheme 1 should be directed to Elsevier

quintet states may be an important prerequisite for its ability to cleave DNA [33]. It was demonstrated that shortwave laser irradiation in the absence of a reducing agent can increase the activity of $[(N4Py)Fe^{II}]^{2+}$ in cutting DNA [35], which is a very important application of transition metal complexes in photodynamic therapy as agents that can be used to cleave DNA [35]. Furthermore, it was shown that in the presence of chromophores, such as 1,8-naphthalimide or 9-aminoacridine, reactive oxygen species scavengers with an additional contribution of photo irradiation can enhance the ability of (**1**) to cut DNA [42]. The research aiming at understanding the reaction mechanism showed that the crucial point in DNA oxidations reactions is the interaction of superoxide radicals with $[(N4Py)Fe^{II}]^{2+}$ to form Fe(III)-peroxo species and/or Fe(III)-hydroperoxide adducts, which are suggested to be the active complexes [43]. Such interaction, due to the ability to carry out both direct and selective DNA cleavage reactions, can contribute to the formation of more active transition metal complexes with *N*-pentadentate ligands, which may be used as synthetic compounds mimicking iron(II)-BLM.

Before SARS-CoV-2, cancer was known to be one of the major causes of death, therefore new substances for chemotherapy drugs are constantly searched for. The iron carbonyl complex $[(N4Py)Fe^{II}(CO)]^{2+}$ connected with a short peptide has strong photo-induced cytotoxicity and and may find application in the treatment of prostate cancer [39]. The $[(N4Py)Fe^{II}(CO)]^{2+}$ complex is stable in an aqueous solution, has an appropriate arrangement of ligand enabling binding with peptides, also shows photo-induced toxicity towards PC-3 cancer cells. Additionally, it can strongly bind CO and is capable of rapid photolytic release of this group

[39]. Moreover, application of N4Py-based iron(II) complexes in the treatment of SKOV-3 and MDA-MB-231 cancer cells showed effective double stranded DNA cleavage, similar to the effect obtained with bleomycin (Scheme 3) [41].

DNA strand breaks resulting from the application of the Fe(II)-N4Py complexes were caused by the triggering of apoptosis preceded by permanent DNA cleavage and oxidative damage to other cellular components. In addition, the ability of these complexes to directly oxidize DNA cleavage was observed [41].

Future prospects and conclusion

Complexes transition metal ions especially iron and/or manganese have become important oxidants in industries. They catalyze the reactions of oxidation of organic compounds with dioxygen or hydrogen peroxide, and reduce the amount of environmentally harmful waste generated. Recent catalytic researches are focused on a significant increase in the efficiency of the catalyzed reactions e.g., by introduction of special reactivity regulators, which should bring benefits to industrial branches. Additionally, complexes of *N*-pentadentate ligands with iron/manganese ions show similarity to natural systems, and may find application as potential drugs. Candidates for new pharmaceuticals should have an appropriate structure for attachment

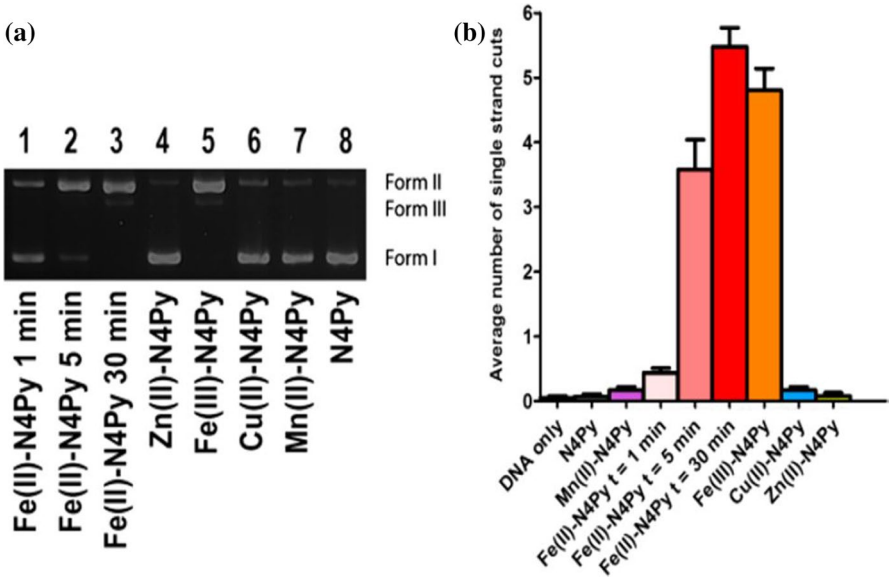

Scheme 2 **a** Gel cleavage analysis, where 1.0 μM complex, 0.1 μg/μL pUC18 plasmid DNA, and 1.0 mM dithiothreitol (DTT) were used in TrisHCl (pH 8.0) at 37 °C. From supercoiled DNA (form I), nicked (form II) and linear (form III) DNA were obtained. After 30 min of incubation only for complexes of Fe(II) and Fe(III) with N4Py traces of supercoiled DNA were observed. **b** Mean number of single strand cleavages according to DNA particle [31]. Reprinted from American Chemical Society, Copyright© 2018, https://pubs.acs.org/doi/10.1021/acs.inorgchem.8b00714, further permissions related to Scheme 2 should be directed to the ACS

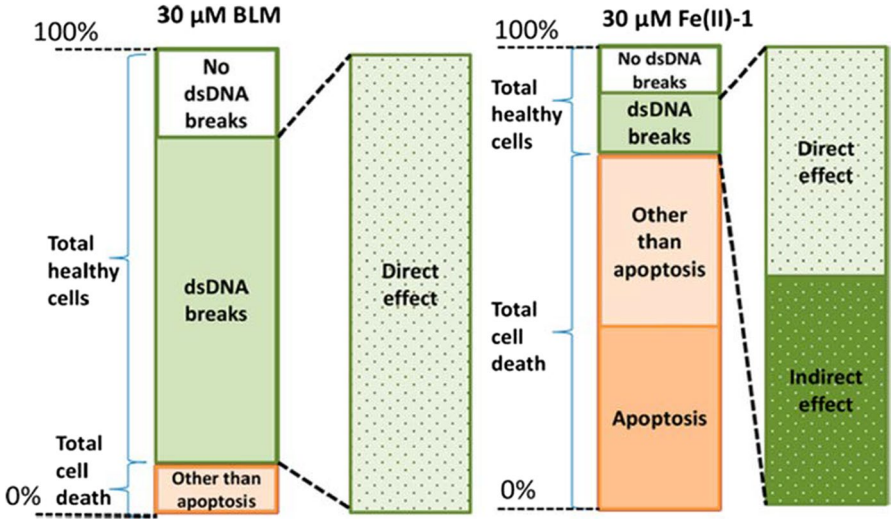

Scheme 3 Variable effect on living cells BLM *vs* N4Py treatment. After 48 h, a different response was obtained with SKOV-3 cells treated with BLM or N4Py. 30 μM BLM causes a large number of double standard DNA (dsDNA) breaks, but more cells die upon treatment with 30 μM N4Py [41]. Reprinted from American Chemical Society, Copyright© 2014, https://pubs.acs.org/doi/10.1021/cb500057n, further permissions related to Scheme 3 should be directed to the ACS

to peptides – this condition is fulfilled by the discussed iron and manganese complexes with N4Py and Bn-TPEN ligands. Nevertheless iron compounds with N4Py have still proved to be more effective in cutting DNA than the corresponding manganese ones. Laser irradiation can intensify the activity of iron(II)-N4Py in cleaving DNA, which is very important for the use of transition metal complexes in photodynamic therapy, as agents that can be used to DNA cleavage. Moreover, the iron carbonyl complex $[(N4Py)Fe^{II}(CO)]^{2+}$ may find application in the treatment of prostate cancer. On the other hand, studies on the use of analogous complexes with the Bn-TPEN ligand in reactions with DNA have not been published yet, which, due to the similarity to N4Py in the way of activating dioxygen, seems to be only a matter of time. This review may contribute to the spread of new application directions for the catalysts based on the skeleton of the described *N*-pentadentate ligands, starting from the synthesis of new drugs, through photodriven water oxidation reaction, finally to their application in sustainable technologies.

References

1. Que L Jr, Ho RYN (1996) Dioxygen activation by enzymes with mononuclear non-heme iron active sites. Chem Rev 96:2607–2624. https://doi.org/10.1021/cr960039f
2. Chen J, Jiang Z, Fukuzumi S, Nam W, Wang B (2020) Artificial nonheme iron and manganese oxygenases for enantioselective olefin epoxidation and alkane hydroxylation reactions. Coord Chem Rev 421(213443):1–28. https://doi.org/10.1016/j.ccr.2020.213443
3. Xu S, Draksharapu A, Rasheed W, Que L Jr (2019) Acid pKa dependence in O−O bond heterolysis of a nonheme Fe^{III}−OOH intermediate to form a potent Fe^{V}=O oxidant with heme compound I-like reactivity. J Am Chem Soc 141:16093–16107. https://doi.org/10.1021/jacs.9b08442
4. Hong YH, Jung J, Nakagawa T, Sharma N, Lee Y-M, Nam W, Fukuzumi S (2019) Photodriven oxidation of water by plastoquinone analogs with a nonheme iron catalyst. J Am Chem Soc 141:6748–6754. https://doi.org/10.1021/jacs.9b02517
5. Wong SD, Bell CB, Liu LV, Kwak Y, England J, Alp EE, Zhao J, Que L Jr, Solomon EI (2011) Nuclear resonance vibrational spectroscopy on the Fe^{IV}=O $S = 2$ non-heme site in TMG_3tren: experimentally-calibrated insights into reactivity. Angew Chem Int Ed Engl 50(14):3215–3218. https://doi.org/10.1002/anie.201007692
6. Collins MJ, Ray K, Que L Jr (2006) Electrochemical generation of a nonheme oxoiron(IV) complex. Inorg Chem 45:8009–8011. https://doi.org/10.1021/ic061263i
7. Lee Y-M, Dhuri SN, Sawant SC, Cho J, Kubo M, Ogura T, Fukuzumi S, Nam W (2009) Water as an oxygen source in the generation of mononuclear nonheme iron(IV) oxo complexes. Angew Chem Int Ed 48:1803–1806. https://doi.org/10.1002/anie.200805670
8. Wang M, Qu Z (2020) The C-H bond activation by non-heme oxidant $[(N4Py)Fe^{IV}(O)]^{2+}$ with external electric field. Theor Chem Acc 64:139–147. https://doi.org/10.1007/s00214-020-2581-4
9. Fukuzumi S (2015) Electron transfer and catalysis with high-valent metal-oxo complexes. Dalton Trans 44:6696–6705. https://doi.org/10.1039/C5DT00204D
10. Kroll N, Speckmann I, Schoknecht M, Gülzow J, Diekmann M, Pfrommer J, Stritt A, Schlangen M, Grohmann A, Hörner G (2019) O-O bond formation and liberation of dioxygen mediated by N5-coordinate non-heme iron(IV) complexes. Angew Chem Int Ed 58:13472–13478. https://doi.org/10.1002/anie.201903902
11. Massie AA, Denler MC, Singh R, Sinha A, Nordlander E, Jackson TA (2020) Structural characterization of a series of N5-ligated MnIV-Oxo species. Chem Eur J 26:900–912. https://doi.org/10.1002/chem.201904434
12. Hitomi Y, Arakawa K, Kodera M (2014) Synthesis, stability and reactivity of the first mononuclear nonheme oxoiron(IV) species with monoamido ligation: a putative reactive species generated from iron-bleomycin. Chem Commun 50:7485–7487. https://doi.org/10.1039/C4CC01409J
13. McDonald AR, Que L Jr (2013) High-valent nonheme iron-oxo complexes: synthesis, structure, and spectroscopy. Coord Chem Rev 257:414–428. https://doi.org/10.1016/j.ccr.2012.08.002
14. Mitra M, Nimir H, Demeshko S, Bhat SS, Malinkin SO, Haukka M, Lloret-Fillol J, Lisensky GC, Meyer F, Shteinman AA, Browne WR, Hrovat DA, Richmond MG, Costas M, Nordlander E (2015) Nonheme Fe(IV) oxo complexes of two new pentadentate ligands and their hydrogen-atom and oxygen-atom transfer reactions. Inorg Chem 54:7152–7164. https://doi.org/10.1021/ic5029564
15. de Sousa DP, Miller CJ, Chang Y, Waite TD, McKenzie CJ (2017) Electrochemically generated *cis*-carboxylato-coordinated iron(IV) oxo acid-base congeners as promiscuous oxidants of water pollutants. Inorg Chem 56:14936–14947. https://doi.org/10.1021/acs.inorgchem.7b02208
16. Chantarojsiri T, Sun Y, Long JR, Chang CJ (2015) Water-soluble iron(IV)-oxo complexes supported by pentapyridine ligands: axial ligand effects on hydrogen atom and oxygen atom transfer reactivity. Inorg Chem 54(12):5879–5887. https://doi.org/10.1021/acs.inorgchem.5b00658
17. Rohde J-U, Torelli S, Shan X, Lim MH, Klinker EJ, Kaizer J, Chen K, Nam W, Que L Jr (2004) Structural insights into nonheme alkylperoxoiron(III) and oxoiron(IV) intermediates by X-ray absorption spectroscopy. J Am Chem Soc 126:16750–16761. https://doi.org/10.1021/ja047667w
18. Saito T, Takano Y (2018) Transition state search using rPM6: iron- and manganese-catalyzed oxidation reactions as a test case. Bull Chem Soc Jpn 91:1377–1389. https://doi.org/10.1246/bcsj.20180119
19. Company A, Sabenya G, González-Béjar M, Gómez L, Clémancey M, Blondin G, Jasniewski AJ, Puri M, Browne WR, Latour J-M, Que L Jr., Costas M, Pérez-Prieto J, Lloret-Fillol J (2014)

Triggering the generation of an iron(IV)-oxo compound and its reactivity toward sulfides by RuII photocatalysis. J Am Chem Soc 136:4624-4633. https://doi.org/10.1021/ja412059c
20. Sahu S, Zhang B, Pollock CJ, Durr M, Davies CG, Confer AM, Ivanović-Burmazović I, Siegler MA, Jameson GNL, Krebs C, Goldberg DP (2016) Aromatic C-F hydroxylation by nonheme iron(IV)-oxo complexes: structural, spectroscopic, and mechanistic investigations. J Am Chem Soc 138:12791-12802. https://doi.org/10.1021/jacs.6b03346
21. Massie AA, Denler MC, Cardoso LT, Walker AN, Hossain MK, Day VW, Nordlander E, Jackson TA (2017) Equatorial ligand perturbations influence the reactivity of manganese(IV)-oxo complexes. Angew Chem Int Ed 56:4178–4182. https://doi.org/10.1002/anie.201612309
22. Que L Jr (2007) The road to non-heme oxoferryls and beyond. Acc Chem Res 40:493–500. https://doi.org/10.1021/ar700024g
23. Solomon EI, Brunold TC, Davis MI, Kemsley JN, Lee S-K, Lehnert N, Neese F, Skulan AJ, Yang Y-S, Zhou J (2000) Geometric and electronic structure/function correlations in non-heme iron enzymes. Chem Rev 100:235–349. https://doi.org/10.1021/cr9900275
24. Nam W (2007) High-valent iron(IV)-oxo complexes of heme and non-heme ligands in oxygenation reactions. Acc Chem Res 40:522–531. https://doi.org/10.1021/ar700027f
25. Sahu S, Goldberg DP (2016) Activation of dioxygen by iron and manganese complexes: a heme and nonheme perspective. J Am Chem Soc 138(36):11410–11428. https://doi.org/10.1021/jacs.6b05251
26. Hicks SD, Kim D, Xiong S, Medvedev GA, Caruthers J, Hong S, Nam W, Abu-Omar MM (2014) Non-heme manganese catalysts for on-demand production of chlorine dioxide in water and under mild conditions. J Am Chem Soc 136:3680–3686. https://doi.org/10.1021/ja5001642
27. Mani B, Natarajan S, Ha H, Lee YH, Nam KT (2018) Involvement of high-valent manganese-oxo intermediates in oxidation reactions: realisation in nature, nano and molecular systems. Nano Convergence 5:18. https://doi.org/10.1186/s40580-018-0150-5
28. Wong E, Jeck J, Grau M, White AJP, Britovsek GJP (2013) A strong-field pentadentate ligand in iron-based alkane oxidation catalysis and implications for iron(IV) oxo intermediates. Catal Sci Technol 3:1116–1122. https://doi.org/10.1039/C3CY20823K
29. Thibon A, England J, Martinho M, Young VG Jr, Frisch JR, Guillot R, Girerd JJ, Münck E, Que L Jr, Banse F (2008) Proton- and reductant-assisted dioxygen activation by a nonheme iron(II) complex to form an oxoiron(IV) intermediate. Angew Chem Int Ed Engl 47(37):7064–7067. https://doi.org/10.1002/anie.200801832
30. Roelfes G, Vrajmasu V, Chen K, Ho RYN, Rohde J-U, Zondervan C, la Crois RM, Schudde EP, Lutz M, Spek AL, Hage R, Feringa BL, Münck E, Que L Jr (2003) End-on and side-on peroxo derivatives of non-heme iron complexes with pentadentate ligands: models for putative intermediates in biological iron/dioxygen chemistry. Inorg Chem 42:2639–2653. https://doi.org/10.1021/ic034065p
31. Geersing A, Segaud N, van der Wijst MGP, Rots MG, Roelfes G (2018) Importance of metal-ion exchange for the biological activity of coordination complexes of the biomimetic ligand N4Py. Inorg Chem 57:7748–7756. https://doi.org/10.1021/acs.inorgchem.8b00714
32. Karges J, Goldner P, Gasser G (2019) Synthesis, characterization, and biological evaluation of red-absorbing Fe(II) polypyridine complexes. Inorganics 7(4):1–15. https://doi.org/10.3390/inorganics7010004
33. Draksharapu A, Li Q, Logtenberg H, van den Berg TA, Meetsma A, Killeen JS, Feringa BL, Hage R, Roelfes G, Browne WR (2012) Ligand exchange and spin state equilibria of Fe^{II}(N4Py) and related complexes in aqueous media. Inorg Chem 51:900–913. https://doi.org/10.1021/ic201879b
34. Wong EL-M, Fang G-S, Che C-M, Zhu N (2005) Highly cytotoxic iron(II) complexes with pentadentate pyridyl ligands as a new class of anti-tumor agents. Chem Commun 2005:4578–4580. https://doi.org/10.1039/B507687K
35. Li Q, Browne WR, Roelfes G (2010) Photoenhanced oxidative DNA cleavage with non-heme iron(II) complexes. Inorg Chem 49:11009–11017. https://doi.org/10.1021/ic1014785
36. Roelfes G, Lubben M, Chen K, Ho RYN, Meetsma A, Genseberger S, Hermant RM, Hage R, Mandal SK, Young VG Jr, Zang Y, Kooijman H, Spek AL, Que L Jr, Feringa BL (1999) Iron chemistry of a pentadentate ligand that generates a metastable Fe^{III}-OOH intermediate. Inorg Chem 38:1929–1936. https://doi.org/10.1021/ic980983p
37. Roelfes G, Lubben M, Leppard SW, Schudde EP, Hermant RM, Hage R, Wilkinson EC, Que L Jr, Feringa BL (1997) Functional models for iron-bleomycin. J Mol Catal A: Chem 117:223–227. https://doi.org/10.1016/S1381-1169(96)00356-1

38. Ho RYN, Roelfes G, Feringa BL, Que L Jr (1999) Raman evidence for a weakened O-O bond in mononuclear low-spin iron(III)-hydroperoxides. J Am Chem Soc 121:264–265. https://doi.org/10.1021/ja982812p
39. Jackson CS, Schmitt S, Dou QP, Kodanko JJ (2011) Synthesis, characterization, and reactivity of the stable iron carbonyl complex [Fe(CO)(N4Py)]$(ClO_4)_2$: photoactivated carbon monoxide release, growth inhibitory activity, and peptide ligation. Inorg Chem 50:5336–5338. https://doi.org/10.1021/ic200676s
40. Chen J, Stubbe J (2005) Bleomycins: towards better therapeutics. Nat Rev Cancer 5:102–112. https://doi.org/10.1038/nrc1547
41. Li Q, van der Wijst MGP, Kazemier HG, Rots MG, Roelfes G (2014) Efficient nuclear DNA cleavage in human cancer cells by synthetic bleomycin mimics. ACS Chem Biol 9:1044–1051. https://doi.org/10.1021/cb500057n
42. Li Q, Browne WR, Roelfes G (2011) DNA cleavage activity of Fe(II)N4Py under photo irradiation in the presence of 1,8-naphthalimide and 9-aminoacridine: unexpected effects of reactive oxygen species scavengers. Inorg Chem 50:8318–8325. https://doi.org/10.1021/ic2008478
43. Li Q, van den Berg TA, Feringa BL, Roelfes G (2010) Mononuclear Fe(II)-N4Py complexes in oxidative DNA cleavage: structure, activity and mechanism. Dalton Trans 39:8012–8021. https://doi.org/10.1039/B927145G
44. Roelfes G, Lubben M, Hage R, Que L Jr, Feringa BL (2000) Catalytic oxidation with a non-heme iron complex that generates a low-spin $Fe^{III}OOH$ intermediate. Eur Chem J 6(12):2152–2159. https://doi.org/10.1002/1521-3765(20000616)6:12%3c2152::aid-chem2152%3e3.0.co;2-o
45. Lehnert N, Neese F, Ho RYN, Que L Jr, Solomon EI (2002) Electronic structure and reactivity of low-SpinFe(III)-hydroperoxo complexes: comparison to activated bleomycin. J Am Chem Soc 124(36):10810–10822. https://doi.org/10.1021/ja012621d
46. van den Berg TA, de Boer JW, Browne WR, Roelfes G, Feringa BL (2004) Enhanced selectivity in non-heme iron catalysed oxidation of alkanes with peracids: evidence for involvement of Fe(IV)=O species. Chem Commun 2550. https://doi.org/10.1039/b412016g
47. Chen J, Draksharapu A, Angelone D, Unjaroen D, Padamati SK, Hage R, Swart M, Duboc C, Browne WR (2018) H_2O_2 oxidation by Fe^{III}-OOH intermediates and its effect on catalytic efficiency. ACS Catal 8:9665–9674. https://doi.org/10.1021/acscatal.8b02326
48. Oloo WN, Meier KK, Wang Y, Shaik S, Münck E, Que L Jr (2014) Identification of a low-spin acylperoxoiron(III) intermediate in bio-inspired non-heme iron-catalysed oxidations. Nat Commun 5:3046–3054. https://doi.org/10.1038/ncomms4046
49. Hazell A, McKenzie CJ, Nielsen LP, Schindler S, Weitze M (2002) Mononuclear non-heme iron(III) peroxide complexes: syntheses, characterisation, mass spectrometric and kinetic studies. J Chem Soc Dalton Trans 310-317. https://doi.org/10.1039/B103844N
50. Klinker EJ, Kaizer J, Brennessel WW, Woodrum NL, Cramer CJ, Que L Jr (2005) Structures of nonheme oxoiron(IV) complexes from X-ray crystallography, NMR spectroscopy, and DFT calculations. Angew Chem Int Ed 44:3690–3694. https://doi.org/10.1002/anie.200500485
51. Kaizer J, Klinker EJ, Oh NY, Rohde J-U, Song WJ, Stubna A, Kim J, Münck E, Nam W, Que L Jr (2004) Nonheme $Fe^{IV}O$ complexes that can oxidize the C-H bonds of cyclohexane at room temperature. J Am Chem Soc 126:472–473. https://doi.org/10.1021/ja037288n
52. Sastri CV, Seo MS, Park MJ, Kim KM, Nam W (2005) Formation, stability, and reactivity of a mononuclear nonheme oxoiron(IV) complex in aqueous solution. Chem Commun 1405-1407. https://doi.org/10.1039/B415507F
53. Hohenberger J, Ray K, Meyer K (2012) The biology and chemistry of high-valent iron-oxo and iron-nitrido complexes. Nat Commun 3:720. https://doi.org/10.1038/ncomms1718
54. Park MJ, Lee J, Suh Y, Kim J, Nam W (2006) Reactivities of mononuclear non-heme iron intermediates including evidence that Iron(III)-hydroperoxo species is a sluggish oxidant. J Am Chem Soc 128:2630–2634. https://doi.org/10.1021/ja055709q
55. Wang D, Zhang M, Bühlmann P, Que L Jr (2010) Redox potential and C-H bond cleaving properties of a nonheme Fe^{IV}=O complex in aqueous solution. J Am Chem Soc 132:7638–7644. https://doi.org/10.1021/ja909923w
56. Kumar D, Hirao H, Que L Jr, Shaik S (2005) Theoretical investigation of C-H hydroxylation by $(N4Py)Fe^{IV}=O^{2+}$: an oxidant more powerful than P450? J Am Chem Soc 127:8026–8027. https://doi.org/10.1021/ja0512428

57. de Visser SP, Oh K, Han A-R, Nam W (2007) Combined experimental and theoretical study on aromatic hydroxylation by mononuclear nonheme iron(IV)-oxo complexes. Inorg Chem 46:4632–4641. https://doi.org/10.1021/ic700462h
58. Que L Jr. (2013) High-valent nonheme iron oxidants in biology: lessons from synthetic Fe^{IV}=O complexes. Bull Jpn Soc Coord Chem 62:30–37. PMCID: PMC4322783
59. Jensen KB, McKenzie CJ, Nielsen LP, Pedersen JZ, Svendsen HM (1999) Deprotonation of low-spin mononuclear iron(III)-hydroperoxide complexes give transient blue species assigned to high-spin iron(III)-peroxide complexes. Chem Commun 1313. https://doi.org/10.1039/A902985K
60. Hong S, Lee Y-M, Shin W, Fukuzumi S, Nam W (2009) Dioxygen activation by mononuclear nonheme iron(II) complexes generates iron-oxygen intermediates in the presence of an NADH analogue and proton. J Am Chem Soc 131:13910–13911. https://doi.org/10.1021/ja905691f
61. Lee Y-M, Kotani H, Suenobu T, Nam W, Fukuzumi S (2008) Fundamental electron-transfer properties of non-heme oxoiron(IV) complexes. J Am Chem Soc 130:434–435. https://doi.org/10.1021/ja077994e
62. Wu AJ, Penner-Hahn JE, Pecoraro VL (2004) Structural, spectroscopic, and reactivity models for the manganese catalases. Chem Rev 104:903–938. https://doi.org/10.1021/cr020627v
63. Leto DF, Ingram R, Day VW, Jackson TA (2013) Spectroscopic properties and reactivity of a mononuclear oxomanganese(IV) complex. Chem Commun 49:5378–5380. https://doi.org/10.1039/C3CC00244F
64. Geiger RA, Leto DF, Chattopadhyay S, Dorlet P, Anxolabéhère-Mallart E, Jackson TA (2011) Geometric and electronic structures of peroxomanganese(III) complexes supported by pentadentate amino-pyridine and -imidazole ligands. Inorg Chem 50:10190–10203. https://doi.org/10.1021/ic201168j
65. Kripli B, Garda Z, Sólyom B, Tircsó G, Kaizer J (2020) Formation, stability and catalase-like activity of mononuclear manganese(II) and oxomanganese(IV) complexes in protic and aprotic solvents. New J Chem 44:5545–5555. https://doi.org/10.1039/C9NJ06004A
66. Yin G (2013) Understanding the oxidative relationships of the metal oxo, hydroxo, and hydroperoxide intermediates with manganese(IV) complexes having bridged cyclams: correlation of the physicochemical properties with reactivity. Acc Chem Res 46(2):483–492. https://doi.org/10.1021/ar300208z
67. Chen J, Lee Y-M, Davis KM, Wu X, Seo MS, Cho K-B, Yoon H, Park YJ, Fukuzumi S, Pushkar YN, Nam W (2013) A mononuclear non-heme manganese(IV)−oxo complex binding redox-inactive metal ions. J Am Chem Soc 135(17):6388–6391. https://doi.org/10.1021/ja312113p
68. Leto DF, Massie AA, Rice DB, Jackson TA (2016) Spectroscopic and computational investigations of a mononuclear manganese(IV)-oxo complex reveal electronic structure contributions to reactivity. J Am Chem Soc 138(47):15413–15424. https://doi.org/10.1021/jacs.6b08661
69. Wu X, Seo MS, Davis KM, Lee Y-M, Chen J, Cho K-B, Pushkar YN, Nam W (2011) A highly reactive mononuclear non-heme manganese(IV)-oxo complex that can activate the strong C-H Bonds of alkanes. J Am Chem Soc 133:20088–20091. https://doi.org/10.1021/ja208523u
70. Morimoto Y, Kotani H, Park J, Lee Y-M, Nam W, Fukuzumi S (2011) Metal ion-coupled electron transfer of a nonheme oxoiron(IV) complex: remarkable enhancement of electron-transfer rates by Sc^{3+}. J Am Chem Soc 133(3):403–405. https://doi.org/10.1021/ja109056x
71. Chen J, Yoon H, Lee Y-M, Seo MS, Sarangi R, Fukuzumi S, Nam W (2015) Tuning the reactivity of mononuclear nonheme manganese(IV)-oxo complexes by triflic acid. Chem Sci 6:3624–3632. https://doi.org/10.1039/C5SC00535C
72. Draksharapu A, Rasheed W, Klein JEMN, Que L Jr (2017) Facile and reversible formation of iron(III)-oxo-cerium(IV) adducts from nonheme oxoiron(IV) complexes and cerium(III). Angew Chem Int Ed Engl 56(31):9091–9095. https://doi.org/10.1002/anie.201704322
73. Draksharapu A, Rasheed W, Klein JEMN, Que L Jr (2017) Facile and reversible formation of iron(III)-oxo-cerium(IV) adducts from nonheme oxoiron(IV) complexes and cerium(III). Angew Chem 129:9219–9223. https://doi.org/10.1002/anie.201704322
74. Mukherjee G, Cantú Reinhard FG, Bagha UK, Sastri CV, de Visser SP (2020) Sluggish reactivity by a nonheme iron(IV)-tosylimido complex as compared to its oxo analogue. Dalton Trans 49:5921–5931. https://doi.org/10.1039/D0DT00018C
75. Rydel-Ciszek K, Pacześniak T, Zaborniak I, Błoniarz P, Surmacz K, Sobkowiak A, Chmielarz P (2020) Iron-based catalytic complexes in preparation of functional materials. Processes 8(12)1683:1–32. https://doi.org/10.3390/pr8121683

76. Zhang Q, Shi B-F (2021) Site-selective functionalization of remote aliphatic C-H bonds *via* C-H metalation. Chem Sci 12:841–852. https://doi.org/10.1039/D0SC05944G
77. Lakk-Bogath D, Speier G, Kaizer J (2015) Oxoiron(IV)-mediated Baeyer-Villiger oxidation of cyclohexanones generated by dioxygen with co-oxidation of aldehydes. N J Chem 39(11):8245–8248. https://doi.org/10.1039/C5NJ02093J
78. Sen K, Creeth A, Metz S (2018) A combined experimental/theoretical approach to accelerated fuel cell development by quantitative prediction of redox potentials. J Power Sources 399:443–447. https://doi.org/10.1016/j.jpowsour.2018.07.056
79. Puri M, Company A, Sabenya G, Costas M, Que L Jr (2016) Oxygen atom exchange between H_2O and non-heme oxoiron(IV) complexes: ligand dependence and mechanism. Inorg Chem 55:5818–5827. https://doi.org/10.1021/acs.inorgchem.6b00023
80. Cho K-B, Shaik S, Nam W (2012) Theoretical investigations into C-H bond activation reaction by Nonheme $Mn^{IV}O$ complexes: multistate reactivity with no oxygen rebound. J Phys Chem Lett 3:2851–2856. https://doi.org/10.1021/jz301241z
81. Kim S, Cho K-B, Lee Y-M, Chen J, Fukuzumi S, Nam W (2016) Factors controlling the chemoselectivity in the oxidation of olefins by nonheme manganese(IV)-oxo complexes. J Am Chem Soc 138:10654–10663. https://doi.org/10.1021/jacs.6b06252
82. Young KJ, Takase MK, Brudvig GW (2013) An anionic N-donor ligand promotes manganese-catalyzed water oxidation. Inorg Chem 52(13):7615–7622. https://doi.org/10.1021/ic400691e
83. Kärkäs MD, Åkermark B (2016) Water oxidation using earth-abundant transition metal catalysts: opportunities and challenges. Dalton Trans 45:14421–14461. https://doi.org/10.1039/C6DT00809G
84. Rydel-Ciszek K, Charczuk M, Pacześniak T, Chmielarz P (2017) Manganese(II) complexes with Bn-tpen as powerful catalysts of cyclohexene oxidation. Chem Pap 71:2085–2093. https://doi.org/10.1007/s11696-017-0201-0
85. Choe C, Yang L, Lv Z, Mo W, Chen Z, Li G, Yin G (2015) Redox-inactive metal ions promoted the catalytic reactivity of non-heme manganese complexes towards oxygen atom transfer. Dalton Trans 44:9182–9192. https://doi.org/10.1039/C4DT03993A
86. Sharma N, Jung J, Lee Y-M, Seo MS, Nam W, Fukuzumi S (2017) Multi-electron oxidation of anthracene derivatives by nonheme manganese(IV)-oxo complexes. Chem Eur J 23:7125–7131. https://doi.org/10.1002/chem.201700666
87. Prakash J, Schmitt SM, Dou QP, Kodanko JJ (2012) Inhibition of the purified 20S proteasome by non-heme iron complexes. Metallomics 4:174–178. https://doi.org/10.1039/C2MT00131D